Materials Advances

ROYAL SOCIETY OF CHEMISTRY

PAPER

View Article Online
View Journal

Cite this: DOI: 10.1039/d5ma01497b

Glycine–proline–hydroxyproline modification improves the affinity of the CEMP1 N-terminal 20-residue peptide to collagen

Yuxiang Sun, *[ab] Yanqian Zhao,[b] Li Xu*[b] and Weibin Sun*[a]

Received 22nd December 2025,
Accepted 26th April 2026

DOI: 10.1039/d5ma01497b

rsc.li/materials-advances

The N-terminal 20 peptide of cementum matrix protein 1 (CEMP1) shows an affinity for hydroxyapatite (HAP) and induces the nucleation of HAP. However, its poor affinity for collagen limits its application in periodontal tissue repair. Here, we found that modifying N20 peptides with a collagen tripeptide composed of glycine–proline–hydroxyproline (GPH) can significantly promote the binding of N20 peptides to type I collagen rapidly and improve the affinity of N20 peptides to bone powder and gingival fibroblasts. In addition, N20 peptides modified with GPH peptides can significantly increase the tightness of self-assembly of type I collagen, while N20 and individual type I collagen peptides only complete self-assembly in a loose stacking manner. Importantly, the modification of GPH does not affect the efficient interaction between N20 peptides and HAP particles. In summary, our research indicates that GPH-modified peptides can significantly improve their affinity to collagen, providing a theoretical basis for further clinical applications of CEMP1-N20 peptides.

1. Introduction

Previous studies have demonstrated that cementum protein 1 (CEMP1) plays a critical role in the mineralization of dental mineralized tissues.[1] CEMP1 is a protein specifically expressed during human dental mineralization, whose structural features enable efficient binding to calcium ions and matrix proteins, thereby modulating the growth of hydroxyapatite (HAP) crystals.[2,3] In addition to the regulatory effects of native and recombinant human CEMP1 on HAP crystal formation, our group and others have reported that a 20-amino-acid peptide corresponding to the N-terminal region of CEMP1 (MGTS STDSQQAGHRRCSTSN, designated N20) can also promote HAP crystal formation *in vitro*.[4,5] However, the absence of a biological targeting motif restricts the further application of the N20 peptide in dental tissue repair.

Interestingly, the organic matrix of dental mineralized tissues is mainly composed of type I collagen fibers.[6] Type I collagen molecules contain highly repetitive amino acid sequences, such as glycine–proline–hydroxyproline (GPH), also known as the collagen tripeptide.[7–9] It has been reported that the GPH tripeptide in the α-chain of collagen provides the structural basis for collagen fiber assembly *via* helical interlocking.[10] In addition, matrix metalloproteinases (MMPs) represent a family of collagenases that can target collagen and facilitate its biodegradation through recognition of proline-rich short peptides.[11,12] Therefore, the collagen-derived tripeptide GPH, which is rich in proline, shows the potential for targeted binding to collagen.[13,14]

Here, we artificially synthesized the N20 peptide (MGTSSTDS QQAGHRR CSTSN-FITC) and the GPH-N20 peptide (G-P-HYP-G-P-HYP-MGTSTSTDSQQA GHRRCSTSN-FITC) by inserting two segments of the GPH collagen tripeptide. The results indicate that the GPH collagen tripeptide can significantly improve the affinity and transient binding ability of N20 peptides to collagen, instead of intervening in its binding performance with HAP. Meanwhile, GPH modification also facilitates the high-affinity binding of peptides to fibroblasts, demonstrating the potential application of GPH modification in a wide range of collagen targeting processes.

2. Materials and methods

2.1. Molecular dynamics simulation

Before simulation, the two peptides were modeled using Avogadro 1.2.0, and N20 and GPH-N20 peptides, and Type I collagen (PDB ID: 1V4F) were docked using AutoDock Vina to select the optimal binding conformation as the initial complex structure for MD simulation.[15,16] The specific operation of simulating

[a] *Department of Periodontology, Nanjing Stomatological Hospital, Medical School of Nanjing University, Nanjing, 210000, P. R. China. E-mail: sunyuxiang@yzu.edu.cn, wbsun@nju.edu.cn*

[b] *Key laboratory of the Jiangsu Higher Education Institutions for Integrated Traditional Chinese and Western Medicine in Senile Diseases Control, School of Traditional Chinese Medicine, Faculty of Medicine, Yangzhou University, Yangzhou, 225009, PR China. E-mail: xulibg@yzu.edu.cn*

using the molecular dynamics software gromacs 2021.6 is as follows. Pdbfixer was used to repair proteins and generate the corresponding parameterized files in the AMBER14SB-PARMBSC1 force field. Then, with the complex as the center, SPC/E water model molecules were added to generate a cubic water box. The corresponding ions (2 Cl^- in the Protein–N20 complex and 2 Cl^- in Protein–GPH–N20 complex) were added to the complex water box to maintain the electrical neutrality of the simulated system. After the system was completed, the conjugate gradient method was used to minimize energy and ensure that the system was fully stable. The canonical ensemble (NVT) and Berendsen hot bath method were used to control the temperature at 298.15 K and simulate 50000 steps with a step size of 2 fs. Then, the isothermal isobaric ensemble (NPT) and Parrinello Rahman pressure control were used to simulate 50 000 steps with a step size of 2 fs at 1 atmosphere. Then, mdrun simulation was performed with a step size of 2 fs and 5×10^6 steps were simulated for a total of 100 ns; MMPBSA was calculated from the simulated data, and finally the obtained data were analyzed and plotted accordingly.

2.2. Peptide preparation and characterization

The sequences of N20 polypeptides and GPH-N20 polypeptides are listed, respectively: (N20:MGTSSTDSQQAGHRRCSTSN-FITC) and (GPH-N20: G-P- HYP-G-P-HYP-MGTSSTDSQQAGHRRCSTSN-FITC). Both of them were labeled using a green fluorescent marker, FITC. The specific synthesis steps were assisted and guided by Hefei Hesheng Biotechnology Co., Ltd (Hefei, China). The synthesised polypeptides were purified and studied using high-performance liquid chromatography and mass spectrometry.[17] The polypeptide powder was dissolved in deionized water, and dithiothreitol was used to prevent cysteine oxidation.

2.3. Electron microscopy analysis

Type I collagen powder (C823256, Shanghai Mackin Biochemical Co., Ltd, China), N20 peptide and GPH-N20 peptide were dissolved in sterile PBS at a concentration of 100 μg mL^{-1}. Then, 5 mL of collagen solution was mixed with 1 mL of N20 peptide solution or 1 mL of GPH-N20 peptide solution. The five mixed solutions were rotated on a room-temperature rotator for 2 hours. Subsequently, the self-assembling peptides and collagen proteins were diluted using ethanol and ultrasound and coated onto transmission electron microscopy (TEM) grids. After air-drying, the samples were examined by selected area electron diffraction under TEM.

2.4. Fluorescence spectroscopy

After incubating N20 and GPH-N20 peptides with gelatin microspheres (88891E, Shanghai Titan Scientific Co., Ltd, China), bone powder (China Yantai Zhenghai Biotechnology Co., Ltd, China), and HAP particles (1306-06-5, Shanghai Mackin Biochemical Co., Ltd, China) for different times, the particles in the mixed solution were precipitated by centrifugation. The fluorescence intensity of the supernatant was measured using a fluorescence spectrophotometer (RF-5301PC, Japan) with an excitation wavelength of 490 nm to evaluate the changes in peptide concentration. The fluorescence intensity at the maximum emission peak of 520 nm was selected and the offline relationship between fluorescence intensity and changes in peptide concentration was calculated. After the corresponding processing conditions, the fluorescence intensity changes of the 520 nm emission peak were analyzed to evaluate the binding ability of the two peptides with gelatin, bone powder, HAP, *etc.*

2.5. Surface plasmon resonance

The CM5 chip was installed according to the standard operating procedure of the Open SPRTM instrument. The analyte was diluted with 1% DMSO and loaded at 20 μL min^{-1}. The specific steps are as follows:

2.5.1. Chip preparation. The activator was prepared by mixing 400 mM EDC and 100 mM NHS immediately prior to injection. The CM5 sensor chip was activated for 420 s with the mixture at a flow rate of 10 μL min^{-1}.

2.5.2. Ligand immobilization. Type I collagen was diluted to 20 μg mL^{-1} in an immobilization buffer, then it was injected into the sample channel Fc2 at a flow rate of 10 μL min^{-1}, and typically resulted in immobilization levels of 13800 RU; the reference channel Fc1 does not need the ligand immobilization step. The chip was deactivated using 1 M ethanolamine hydrochloride at a flow rate of 10 μL min^{-1} for 420 s.

2.5.3. Running analyte by the multi-cycle method. GPH-N20 was diluted with the same analyte buffer to 8 concentrations (500, 250, 125, 62.5, 31.3, 15.6, 6.8 and 0 μM). GPH-N20 was injected into channel Fc1–Fc2 at a flow rate of 20 μL min^{-1} for an association phase of 100 s, followed by 180 s dissociation. The association and dissociation processes were all performed using the analyte buffer. Complete eight analyte cycles in ascending order of concentration. Chip regeneration was performed immediately after each binding cycle to restore the sensor surface for the next run.

2.6. Cell culture and flow cytometry

Human gingival fibroblasts (HGFs) were cultured in DMEM-H medium containing 10% fetal bovine serum, streptomycin (100 μg mL^{-1}), and penicillin (100 U mL^{-1}). Cells were routinely maintained at 37 °C in humidified air containing 5% CO_2, and passaged once in 1–2 days. HGFs (10^6) were treated with N20 (1 μg mL^{-1}) and GPH-N20 (1 μg mL^{-1}) for 10 min, 30 min, 60 min, respectively. All cells were collected by centrifugation at 1000 rpm for 5 min, washed twice with PBS, and then re-suspended in 500 μL PBS per tube, and the intensity of FITC-labeled cells was detected by flow cytometry.

2.7. Fluorescence microscopy observation

After the bone powder and HAP were incubated with peptides and centrifuged, they were thoroughly washed with PBS and centrifuged again to remove the supernatant. Then, 500 μL of PBS was taken to resuspend the bone powder or HAP, and surgical forceps were used to pick up the bone powder particles and place them on a glass slide. The changes in green fluorescence exhibited by the bone powder were observed. In addition, after replacing the HAP particles, 10 μL of the re-suspended droplets was added onto the loaded fragments, and the changes

in green fluorescence on the HAP particles were observed using a microscope (EVOS FLoid, Thermo Fisher Scientific, USA).

2.8. Statistical analysis

All experimental data are expressed as the mean ± standard deviation (SD). Unless otherwise specified, all experiments were performed in triplicate to ensure reproducibility. Statistical comparisons between different groups were conducted using Student's *t*-test (for two-group comparisons) and one-way analysis of variance (ANOVA) followed by a *post hoc* test (for multiple-group comparisons). Statistical significance was defined as $*p < 0.05$, $**p < 0.01$, and $***p < 0.001$.

3. Results and discussion

3.1. Molecular simulation to show the potential affinity of GPH-modified N20 to collagen

Fig. 1A depicts the mechanism by which the N-terminal 20-residue segment of CEMP1 (denoted as N20) acquires the enhanced high-affinity binding to collagen after modification with the GPH tripeptide. To characterize the binding properties of the two peptides toward collagen, molecular dynamics simulations were performed. Root-mean-square deviation (RMSD), defined as the root-mean-square distance between matched atoms following structural alignment, is commonly utilized to assess the structural stability and conformational drift of a molecule during simulation.[18] Lower RMSD values generally correspond to more stable molecular conformations. As presented in Fig. 1C, GPH-N20 exhibited noticeably smaller RMSD fluctuations than unmodified N20 during the initial 50 ns of binding with the collagen, despite the two peptides showing comparable dynamic profiles in their free states (Fig. 1B). After complex formation, the GPH-N20/collagen system also maintained a lower overall RMSD value, indicative of superior structural stability (Fig. 1D).

To further characterize the dynamic behavior of the complexes, root-mean-square fluctuation (RMSF) analysis was carried out. RMSF quantifies the time-averaged atomic displacement relative to a reference structure over the entire simulation trajectory, thereby reflecting regional flexibility.[19] Higher RMSF values signify greater structural flexibility, whereas lower values imply increased rigidity. The GPH-N20/collagen complex exhibited markedly reduced flexibility compared to the N20/collagen system, implying the formation of a more rigid and stable assembly (Fig. 1E). In parallel, the radius of gyration (R_g) was analyzed to evaluate the overall compactness and folding integrity of the

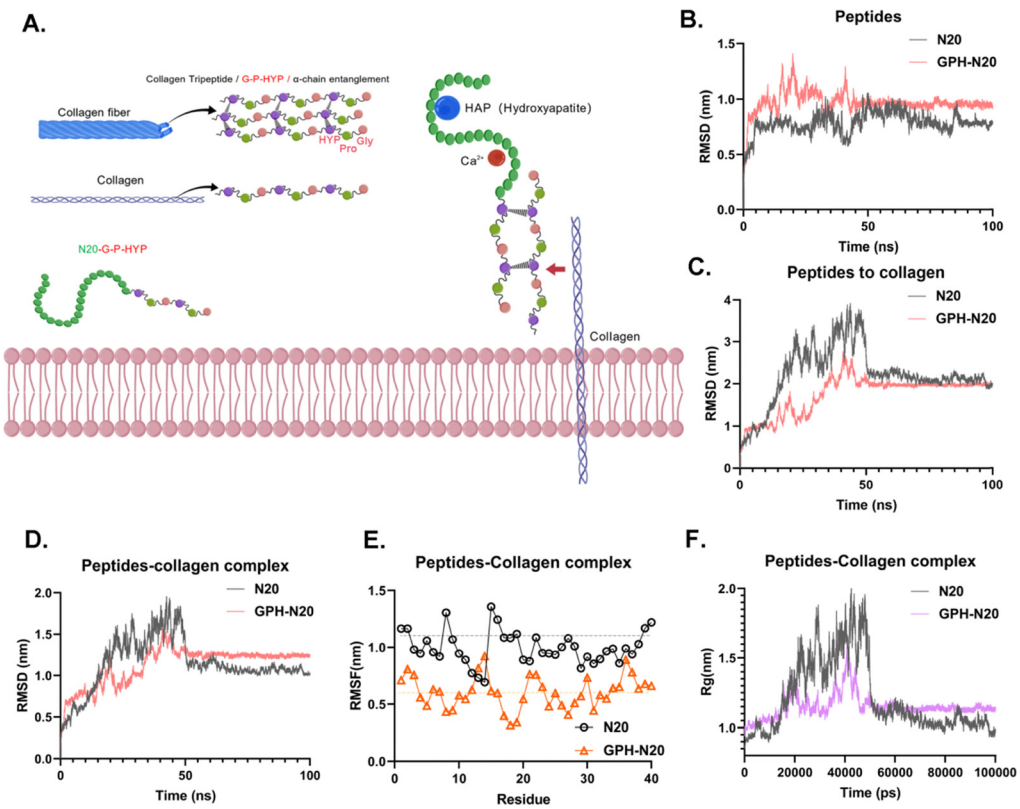

Fig. 1 Molecular simulation to show the potential affinity of GPH-modified N20 to collagen. (A) Schematic diagram illustrating that the N-terminal 20-amino-acid peptide of CEMP1 (N20) modified with the collagen tripeptide (glycine–proline–hydroxyproline, GPH) can enhance the high-affinity binding to collagen. Molecular dynamics simulation calculations were performed based on N20, GPH-N20 and type I collagen. (B) Root mean square deviation (RMSD) data of the two peptides. (C) RMSD data of the two peptides during their binding to collagen. (D) RMSD data of the two peptides after forming complexes with collagen. (E) Root mean square fluctuation (RMSF) values of the two peptides after forming complexes with collagen. (F) Radius of gyration (R_g) values of the two peptides after forming complexes with collagen.

complexes, where R_g represents the mass-weighted root-mean-square distance of all atoms from the molecular center of mass.[20] Smaller R_g values correspond to more compact molecular architectures. Although both complexes underwent dynamic fluctuations, the GPH-N20/collagen system displayed a narrower range of R_g variations, consistent with a more stable and compact conformation (Fig. 1F).

Furthermore, MM-PBSA (Molecular Mechanics/Poisson–Boltzmann Surface Area) calculations were performed to determine the binding free energy between each peptide and collagen (Fig. S1). The results clearly showed that GPH-N20 possessed a significantly stronger binding affinity toward collagen than the unmodified N20 peptide. Notably, hydrogen bond analysis revealed no significant difference in the number of hydrogen bonds formed between the two peptides and collagen (Fig. S2). These observations suggest that the improved collagen-binding affinity of GPH-N20 is likely modulated by a combination of multiple noncovalent interactions rather than hydrogen bonding alone.

3.2. GPH modification supports the affinity of N20 peptides to gelatin

We synthesized FITC-labeled N20 and GPH-N20 peptides, whose molecular weights were verified by mass spectrometry (Fig. S3). HPLC analysis confirmed that the purity of both peptides exceeded 98% (Fig. S4). Fluorescence spectroscopic measurements of aqueous peptide solutions exhibited a maximum emission wavelength at approximately 520 nm upon excitation at 490 nm, and the fluorescence intensity showed a good linear correlation with peptide concentration (Fig. S5).

To validate the enhanced collagen-binding affinity of GPH-N20, the two peptides were separately co-incubated with equivalent amounts of collagen microspheres. After 1 hour of static incubation, peptide binding to gelatin microspheres was assessed by measuring the decrease in peptide concentration *via* fluorescence intensity of the supernatant. Under static conditions, both peptides exhibited comparable reductions in concentration (Fig. 2A). In contrast, under continuous rotational conditions, the concentration of N20 remained almost unchanged, while the concentration of GPH-N20 decreased sharply to nearly one-third within 10 minutes. These results indicate that GPH modification markedly strengthens the binding capacity of N20 to collagen under dynamic, non-static conditions (Fig. 2B). For intuitive visualization, fluorescence imaging was conducted on the microspheres after 10 minutes of incubation. Consistent with the above results, N20 showed negligible binding to gelatin under rotation, whereas GPH-N20 yielded a prominent enhancement in fluorescence intensity on the microsphere surface (Fig. 2C).

3.3. GPH modification supports the affinity of N20 peptides to collagen and fibroblast cells

On the basis of previous analysis, we hypothesized that GPH-N20 might engage in specific binding interactions with collagen

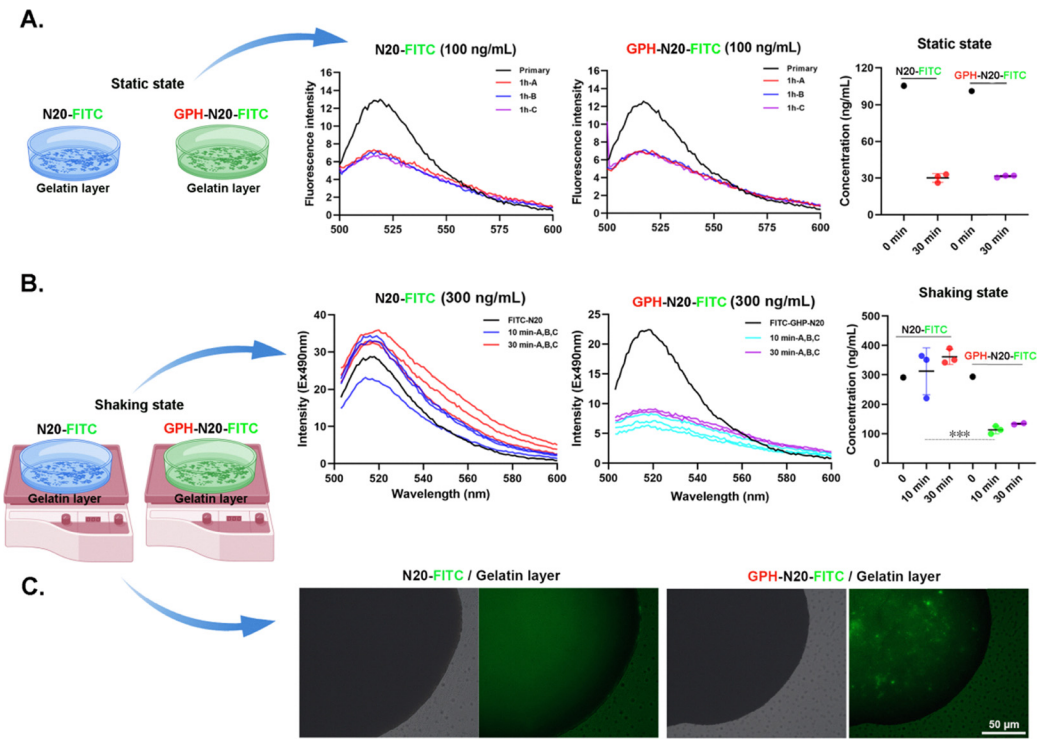

Fig. 2 GPH modification supports the affinity of N20 peptides to gelatin. (A) The two peptides (0.1 μg mL^{-1}) were incubated with commercial gelatin microspheres for 30 min, followed by centrifugation at 1000 rpm for 5 min. The supernatant was collected for fluorescence spectroscopy analysis, and the changes in peptide concentration in the solution before and after incubation were calculated (n = 3). (B) The two peptides (0.5 μg mL^{-1}) were incubated with gelatin microspheres on a rotary incubator for 10 min and 30 min, respectively. The mixtures were centrifuged at 1000 rpm for 5 min, the supernatant was collected for fluorescence spectroscopy analysis, and the changes in peptide concentration in the solution before and after incubation were calculated (n = 3). (C) The microspheres were collected from the 30-min incubation group in (B) and observed under a fluorescence microscope (n = 3). ***, $p < 0.001$, significant difference.

through distinct structural domains (Fig. 3A). To substantiate the high-affinity collagen binding conferred by GPH modification, we employed surface plasmon resonance (SPR) technology to characterize the kinetic interactions between GPH-N20 and type I collagen.[21,22] As illustrated in Fig. 3B, unmodified N20 failed to exhibit any detectable interaction with type I collagen across a broad concentration gradient (ranging from 6.8 μM to 500 μM). In stark contrast, GPH-N20 displayed robust and concentration-dependent binding affinity for collagen with an affinity constant of 42 μM (Fig. S6).

Meanwhile, the self-assembly behavior of type I collagen and the peptides in PBS was observed by transmission electron microscopy (TEM). Individual type I collagen, N20, and GPH-N20 could spontaneously assemble into loose, stacked fibrous structures in PBS (Fig. 3C). However, the mixture of N20 and type I collagen did not change the loose self-assembly structure of collagen. In contrast, the combination of GPH-N20 and type I collagen markedly increased the compactness of the self-assembled fibers, suggesting that GPH modification strengthens the interaction between N20 and collagen (Fig. 3C).

To further evaluate the binding affinity towards bone tissue, the peptides were incubated with bone powder for varying time points. As early as 1 minute, no discernible fluorescence signal was detected on the bone powder surface for either peptide (Fig. 3D). After 10 minutes of incubation, a strong fluorescence signal was exclusively observed for GPH-N20. Even at 60 minutes, N20 only exhibited a weak signal, whereas GPH-N20 maintained an intense and uniform fluorescence signal, revealing that GPH modification significantly enhances the binding affinity and avidity of N20 for bone collagen (Fig. 3D).

Dental fibroblasts represent the most abundant cell type responsible for synthesizing extracellular matrix collagen and are the primary cells involved in periodontal ligament fiber formation, thereby playing a pivotal role in periodontal tissue

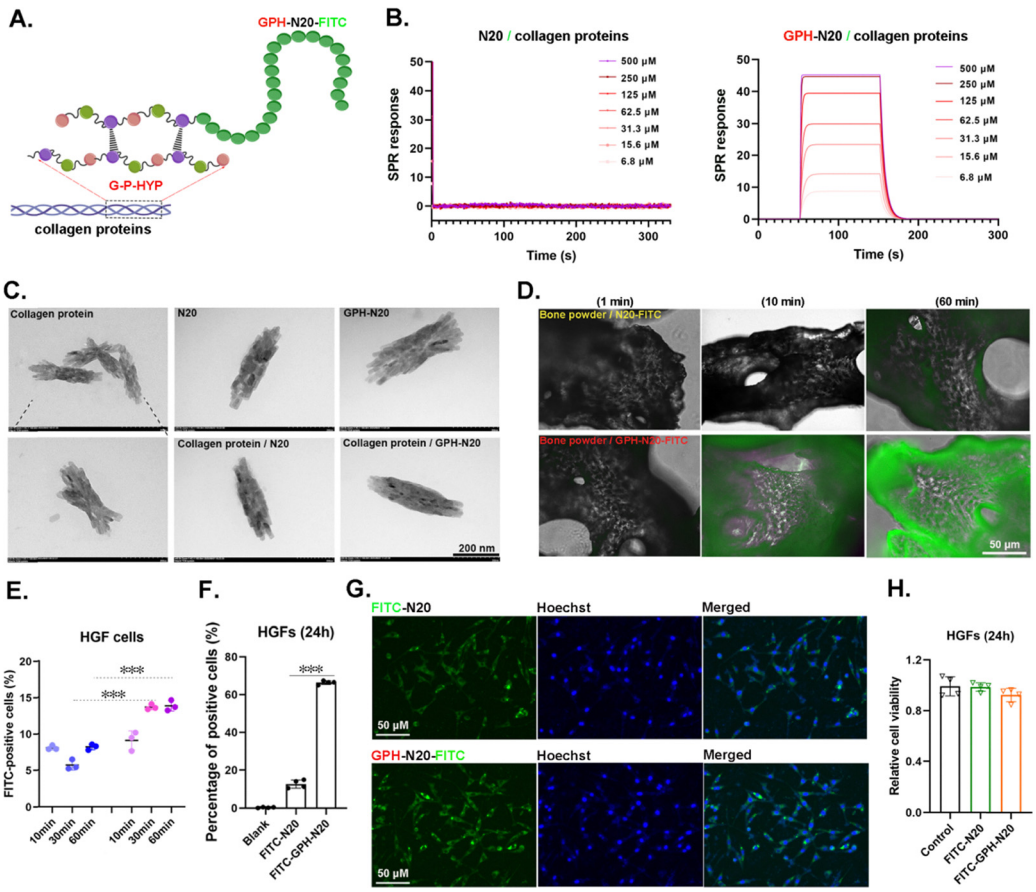

Fig. 3 GPH modification supports the affinity of N20 peptides to collagen and fibroblast cells. (A) Schematic diagram illustrates the principle that collagen tripeptide of GPH can support the binding of N20 peptides to collagen. (B) Based on surface plasmon resonance (SPR) technology, a CM5 chip was used to detect the affinity of the N20 peptide and GPH-N20 peptide for interaction with type I collagen, respectively. (C) The type I collagen, N20, GPH-N20 and protein self-assembly in collagen peptide blends were detected by transmission electron microscopy (TEM). (D) The N20 peptide and GPH-N20 peptide at 0.5 μg mL^{-1} were co-incubated with commercial bone powder under rotating conditions, and then centrifuged after 1 min, 10 min and 30 min to remove the solution. After thorough washing with PBS, the fluorescence signals on the surface of the bone powder were observed using a fluorescence microscope (n = 3). (E) HGFs were cultured and co-incubated with 1 μg mL^{-1} of the two peptides for 10, 30 and 60 min, respectively. After washing, the green fluorescence signals on the cell surface were detected by flow cytometry (n = 3). (F) HGFs were cultured and co-incubated with 1 μg mL^{-1} of the two peptides for 24 h, respectively. After washing, the green fluorescence signals in HGFs were detected by flow cytometry (n = 4). (G) Their green fluorescence signals in HGFs were observed using a fluorescence microscope (n = 4). (H) After HGFs were treated with N20 and GPH-N20, respectively, for 24 h, their relative cell viability was detected by the CCK-8 assay (n = 4). ***, $p < 0.001$, indicating a significant difference.

maintenance and repair.[23] We thus investigated the cell-binding efficiency of the peptides in human gingival fibroblasts (HGFs). Flow cytometric analysis revealed that, within 60 minutes of incubation, N20 failed to increase the positive cell rate (Fig. S7 and Fig. 3E). In contrast, GPH-N20 induced a substantial increase in the positive cell rate as early as 30 minutes. Furthermore, after 24 hours of treatment, the positive rate for N20 was merely ~14%, which was significantly lower than that of GPH-N20 (~67%) (Fig. S8 and Fig. 3F). These observations were further validated by fluorescence microscopy imaging (Fig. 3G), confirming the superior cell-binding capacity of GPH-N20. Importantly, cell viability assays confirmed that both peptides exhibit excellent biocompatibility, thereby validating their potential for biomedical applications (Fig. 3H).

3.4. GPH modification shows no impact on the binding between N20 peptide and HAP

While the collagen-affinity capacity of the CEMP1-derived N20 peptide is critical for facilitating intrafibrillar mineralization, it remains essential to clarify whether GPH modification impacts the binding ability of N20 to hydroxyapatite (HAP). To address this critical question, we designed experiments to evaluate the binding of N20 and GPH-N20 to HAP under both static and rotating conditions (Fig. 4A). The binding efficiency of the peptides to HAP particles was quantified by measuring the residual fluorescence intensity of the supernatant following co-incubation. As shown in Fig. 4B and C, both peptides exhibited a similar decreasing trend in the fluorescence intensity of the supernatant under both static and rotating conditions, with no statistically significant difference observed between the two groups. To further confirm these findings, HAP particles incubated under rotating conditions were collected by centrifugation and visualized *via* fluorescence microscopy. At 10, 30, and 60 minutes of incubation, both peptides generated strong fluorescence signals on the HAP surface, and there was no significant discrepancy in the fluorescence intensity between the N20 and GPH-N20 groups, further indicating that GPH modification does not impair the binding capacity of N20 to HAP (Fig. 4D).

As a core component of dental bone and periodontal tissues, the intrafibrillar bio-mineralization process of collagen fibers directly determines the quality and efficiency of tissue repair.[24]

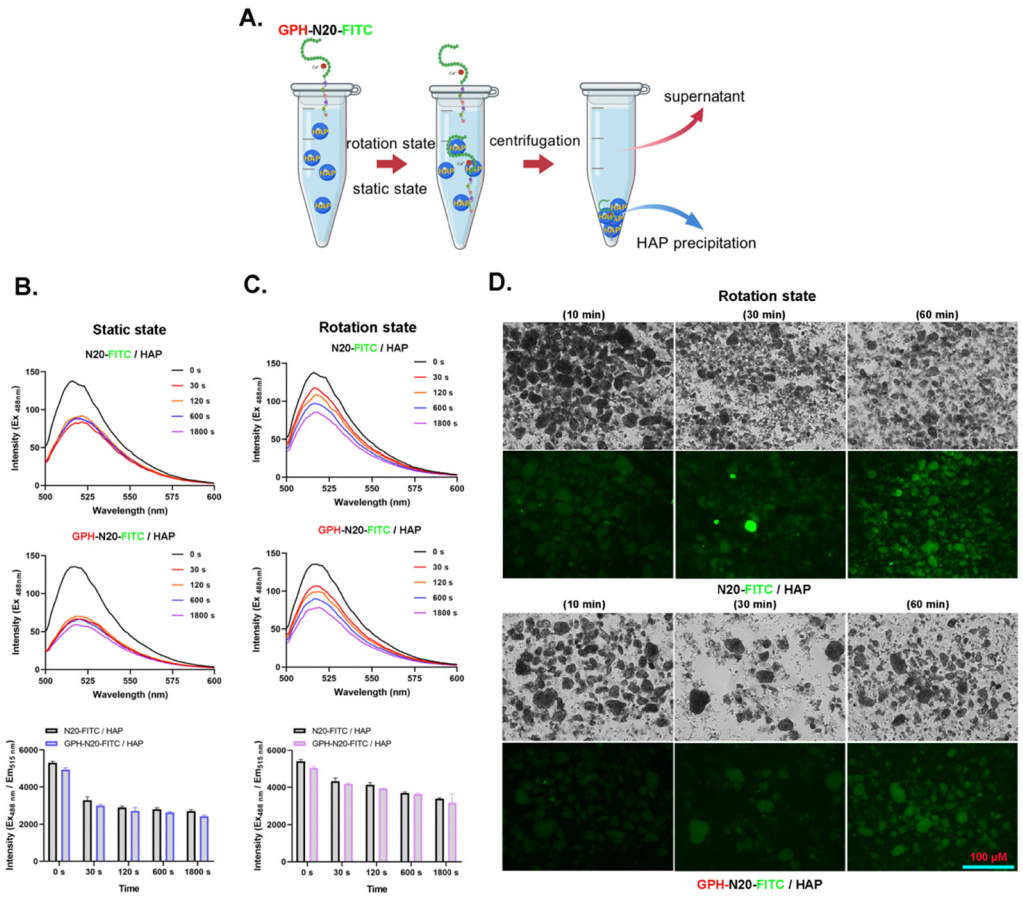

Fig. 4 GPH modification shows no impact on the binding between the N20 peptide and HAP. (A) Schematic diagram illustrates the experimental design; HAP particles were added into the EP tube, followed by the addition of 1 μg mL^{-1} N20 and GPH-N20. The mixtures were shaken on a rotary table or kept at rest for different durations, after which all tubes were centrifuged. The supernatant was used for fluorescence intensity measurement, while the precipitate was used for microscopic observation. (B) and (C) The two peptides at a concentration of 1 μg mL^{-1} were incubated with commercial HAP particles for 30, 120, 600 and 1800 seconds, respectively, and then centrifuged at 1000 rpm for 5 min. The supernatant was collected for fluorescence spectroscopy, and the decrease in the green fluorescence signal in the solution at different time points was calculated. (D) The precipitates centrifuged at different time points in (A) were collected and observed under a fluorescence microscope.

Therefore, improving the intrafibrillar bio-mineralization of collagen fibers is of crucial clinical significance for promoting dental bone repair and periodontal tissue regeneration.[25,26] As the key functional protein in cementum, CEMP1 has been reported to regulate the morphology, chemical composition and deposition of HAP crystals, thereby participating in cementum formation and mineralization.[27] Interestingly, Higinio Arzate *et al.* confirmed that the N20 peptide of CEMP1 retains the partial functions of its parent protein, also exhibiting a strong affinity for HAP and inducing the nucleation of HAP crystals, providing an important theoretical basis for the subsequent development of N20 peptides.[4]

In our previous studies on CEMP1-derived biomimetic peptides, we found that when using such peptides to promote collagen fiber mineralization, those without targeting ability can hardly act precisely inside collagen fibers even if they bind to HAP, and fail to significantly improve the intrafibrillar bio-mineralization process, thus limiting their therapeutic efficacy in dental bone repair.[5] Existing studies have shown that the GPH tripeptide in the α-chain of type I collagen is a key site for the formation of the helical structure and intermolecular cross-linking of bone collagen molecules, as well as the core basis for facilitating collagen fiber assembly and formation.[7,10] Meanwhile, numerous studies have confirmed that collagen tripeptides, as small-molecule fragments of collagen, possess excellent biocompatibility and bioactivity and can promote the growth and repair of bone and cartilage tissues by regulating cell proliferation, differentiation and other processes.[28,29] For example, Hata S *et al.* demonstrated that oral administration of collagen tripeptides in rats with bone defects could induce granulation tissue hyperplasia, facilitate robust osteoblast proliferation and markedly accelerate bone healing. These findings further validate the promising application potential of collagen tripeptides in bone repair.[30] In addition, evidence has revealed that the triple-helix hybridization properties mediated by GPH confer the potential for targeted binding to collagen, and these properties have been harnessed to enhance the collagen-targeting capability of biologics and nanoparticles.[13] Thus, to enhance the mineralization-promoting capacity of N20 peptides, collagen-targeting ability should be introduced while preserving their binding capacity to HAP.

Against the above research background, this study designed a GPH tripeptide modification strategy to endow the N20 peptide with collagen affinity. Experimental results showed that this modification significantly improved the rapid binding ability of N20 peptide to type I collagen, enabling precise targeting to collagen fibers. More importantly, detection revealed that this unstructured modification did not affect the efficient interaction between GPH-N20 and HAP. Although GPH modification has shown promising application potential, its subsequent translation still requires further in-depth systematic research, especially the regulatory effect of the number of GPH repeating units on collagen affinity. The fibrillogenesis of natural collagen relies on the tandem arrangement and synergistic interaction of numerous GPH sequences. Although the two-segment GPH modification strategy adopted in this study has achieved efficient collagen targeting, the number of repeats may not represent the optimal combination. In addition, the conjugation process of GPH modules with functional polypeptides and bioactive molecules also deserves focused optimization. In the initial design of this project, we attempted single-segment GPH modification (GPH1-N20) to reduce the difficulty of polypeptide synthesis. However, the results showed that this scheme significantly increased the pressure of product purification. We speculate that the main reason is that after single-segment GPH modification, the hydrophilicity/hydrophobicity and molecular weight of the polypeptide differ slightly from those of the parent N20 polypeptide, making efficient separation difficult. Therefore, for future clinical applications, it is urgent to develop a simpler, stable and easily purifiable preparation process for GPH conjugation.

Of note, any biomaterial must first meet the requirements of biosafety and immunocompatibility before clinical translation. Therefore, before the GPH-modified N20 polypeptide is further applied in dental bone tissue repair and regeneration, systematic *in vitro* and *in vivo* evaluations still need to be conducted to comprehensively and rigorously verify key issues such as its biosafety, immunogenicity, long-term toxicity and *in vivo* biological effects, so as to lay a reliable foundation for subsequent clinical translation.[31]

4. Conclusions

In short, we found that (1) GPH modification significantly enhances the binding ability of N20 to collagen proteins: N20 modified with GPH (GPH-N20) can bind to type I collagen more quickly and efficiently, solving the problem of poor affinity of the original N20 for collagen. (2) GPH-N20 enhances interactions with bone powder, gingival fibroblasts and the tightness of collagen self-assembly. Compared with N20, GPH-N20 has improved adsorption capacity to bone powder and adhesion ability to gingival fibroblasts. In addition, it can significantly increase the tightness of type I collagen self-assembly, whereas N20 and individual collagen can only achieve self-assembly through loose stacking. (3) GPH modification does not affect the original interaction between N20 and HAP. The modified GPH-N20 retains the high-affinity of N20 to HAP. Thus, GPH modification of N20 peptides not only enhances the high-affinity binding to collagen but also maintains their key characteristic of interacting with HAP, laying a better foundation for their potential application in clinical periodontal tissue repair.

Author contributions

Research design: Yuxiang Sun and Li Xu. Experimental tests and data analysis: Yuxiang Sun and Li Xu. Cellular experiments and data analysis: Yanqian Zhao. Manuscript writing and editing: Yuxiang Sun, Li Xu, and Weibin Sun.

Conflicts of interest

The authors declare that they have no known competing financial interests or personal relationships that could have appeared to influence the work reported in this paper.

Data availability

All data used and required are summarized. Additional data (*e.g.*, raw experimental data, detailed spectral analysis or others) can be obtained from the corresponding author upon reasonable request.

Supplementary information (SI) is available. See DOI: https://doi.org/10.1039/d5ma01497b.

Acknowledgements

This project was funded in part by the National Natural Science Foundation of China (82400583 and 82500600), the Natural Science Foundation of Jiangsu Province (BK20240922), the Nanjing Stomatological Hospital Postdoctoral Fund (202362815), the Research Launch Fund of Yangzhou University (137012813 and 137013058), and the Lvyang Jinfeng Plan for Excellent Doctor of Yangzhou City (137013059 and 137013058). This project was supported by the Open Research Fund of Key Laboratory of Biomarkers and *In Vitro* Diagnosis Translation of Zhejiang province (2022E10024).

References

1 R. Correa, J. Arenas, G. Montoya, L. Hoz, S. López, F. Salgado, R. Arroyo, N. Salmeron, E. Romo, M. Zeichner-David and H. Arzate, *FASEB J.*, 2019, **33**, 1167–1178.
2 X. F. Chen, Y. Liu, J. Yang, W. L. Wu, L. Y. Miao, Y. J. Yu, X. B. Yang and W. B. Sun, *Mater. Sci. Eng., C*, 2016, **59**, 384–389.
3 M. Komaki, K. Iwasaki, H. Arzate, A. S. Narayanan, Y. Izumi and I. Morita, *J. Cell. Physiol.*, 2012, **227**, 649–657.
4 G. Montoya, R. Correa, J. Arenas, L. Hoz, E. Romo, R. Arroyo, M. Zeichner-David and H. Arzate, *J. Pept. Sci.*, 2019, **25**, e3211.
5 L. Mei, Y. Wang, H. Zheng, X. Xing and W. Sun, *Sci. Rep.*, 2025, **15**, 27730.
6 M. G. Kim, J. H. Lee, G. C. Kim, D. S. Hwang, C. H. Kim, B. J. Kim, J. H. Kim and U. K. Kim, *Maxillofac. Plast. Reconstr. Surg.*, 2021, **43**, 17.
7 P. Li and G. Y. Wu, *Amino Acids*, 2018, **50**, 29–38.
8 N. A. Ihoeghian and Q. Shao, *Supramol. Mater.*, 2025, **4**, 100103.
9 V. Sagar, X. J. Ng, L. Lechel, A. C. Rajwar, H. Bargel and A. A. Jalan, *Adv. Funct. Mater.*, 2026, e28087.
10 M. K. Gordon and R. A. Hahn, *Cell Tissue Res.*, 2010, **339**, 247–257.
11 A. Jablonska-Trypuc, M. Matejczyk and S. Rosochacki, *J. Enzyme Inhib. Med. Chem.*, 2016, **31**, 177–183.
12 J. L. Lauer-Fields, D. Juska and G. B. Fields, *Biopolymers*, 2002, **66**, 19–32.
13 T. Z. Luo and K. L. Kiick, *Bioconjugate Chem.*, 2017, **28**, 816–827.
14 P. J. Stahl and S. M. Yu, *Soft Matter*, 2012, **8**, 10409–10418.
15 I. J. D. Nascimento, T. M. de Aquino and E. F. da Silva, *Recent Adv. Inflammation Allergy Drug Discovery*, 2021, **15**, 80–86.
16 O. Trott and A. J. Olson, *J. Comput. Chem.*, 2010, **31**, 455–461.
17 D. V. Anirban Das, Sharad Gupta, Dhiraj Bhatia and Abhijit Biswas, *Supramol. Mater.*, 2025, 100123.
18 R. Brüschweiler, *Proteins*, 2003, **50**, 26–34.
19 M. Amir, S. Shafi, S. Parveen, A. A. Reshi and A. Ahmad, *Pharmaceuticals*, 2024, **17**, 1090.
20 A. Kobayashi, M. Nakajima, Y. Noguchi, R. Morikawa, Y. Matsuo and M. Takasu, *Life*, 2023, **13**, 578.
21 H. Bonnet, L. Coche-Guérente, E. Defrancq, N. Spinelli, A. Van der Heyden and J. Dejeu, *Anal. Chem.*, 2021, **93**, 4134–4140.
22 J. Matsui, K. Akamatsu, N. Hara, D. Miyoshi, H. Nawafune, K. Tamaki and N. Sugimoto, *Anal. Chem.*, 2005, **77**, 4282–4285.
23 V. Pivodova, J. Frankova and J. Ulrichova, *Biomed. Pap.*, 2011, **155**, 109–116.
24 W. X. Mao, X. Y. Li, A. He, M. Ding, Y. Zhang, Z. Dai, Q. Li, W. J. Xiu, Y. L. Hu, Y. B. Mou, D. L. Yang and H. Dong, *Exploration*, 2026, **6**, 20240315.
25 J. Moradian-Oldak and A. George, *J. Dent. Res.*, 2021, **100**, 1020–1029.
26 M. M. Hou, N. N. Shi, Y. J. Guo, J. Z. Tang, H. Peng, B. Y. Liang, Y. X. Yu, C. G. Yi and H. C. Li, *Exploration*, 2026, **6**, 20250031.
27 Q. Q. Wang, L. Y. Miao, H. Zhang, S. Q. Wang, Q. L. Li and W. B. Sun, *J. Mater. Chem. B*, 2020, **8**, 2350–2362.
28 L. W. Li, L. L. Zhang, K. X. Zheng, T. D. Xiong, W. Yang, K. N. Yang, Y. Zhuang, L. Z. Qiu, Y. Y. Chen and J. W. Dai, *Adv. Funct. Mater.*, 2026, e28087.
29 K. H. Leem, S. Kim, J. Lim, H. J. Park, Y. C. Shin and J. S. Lee, *J. Med. Food*, 2023, **26**, 809–819.
30 N. Tsuruoka, R. Yamato, Y. Sakai, Y. Yoshitake and H. Yonekura, *Biosci., Biotechnol., Biochem.*, 2007, **71**, 2680–2687.
31 Y. Dai, J. Chen and W. Guo, *Eur. Cells Mater.*, 2024, **47**, 190–218.